Available online at www.sciencedirect.com
ScienceDirect
Thermochimica Acta 457 (2007) 20–26
thermochimica acta
www.elsevier.com/locate/tca

Thermodynamic investigation of several natural polyols (I): Heat capacities and thermodynamic properties of xylitol

Bo Tong [a,c], Zhi-Cheng Tan [a,b,*], Quan Shi [a,c], Yan-Sheng Li [b], Dan-Ting Yue [a], Shao-Xu Wang [b]

[a] *Thermochemistry Laboratory, Dalian Institute of Chemical physics, Chinese Academy of Sciences, Dalian 116023, China*
[b] *College of Environmental Science and Engineering, Dalian Jiaotong University, Dalian 116028, China*
[c] *Graduate School of the Chinese Academy of Sciences, Beijing 100049, China*

Received 7 July 2006; received in revised form 27 February 2007; accepted 27 February 2007

Abstract

The low-temperature heat capacity $C^0_{p,\mathrm{m}}$ of xylitol was precisely measured in the temperature range from 80 to 390 K by means of a small sample automated adiabatic calorimeter. A solid–liquid phase transition was found from the experimental C_p–T curve in the temperature range 360–375 K with the peak heat capacity at 369.04 K. The dependence of heat capacity on the temperature was fitted to the following polynomial equations with least square method. In the temperature range of 80–360 K, $C^0_{p,\mathrm{m}}(\mathrm{J\,K^{-1}\,mol^{-1}}) = 165.87 + 105.19x + 1.8011x^2 - 41.445x^3 - 41.851x^4 + 65.152x^5 + 66.744x^6$, $x = [T(\mathrm{K}) - 220]/140$. In the temperature range of 370–390 K, $C^0_{p,\mathrm{m}}(\mathrm{J\,K^{-1}\,mol^{-1}}) = 426.19 + 5.6366x$, $x = [T(\mathrm{K}) - 380]/10$. The molar enthalpy and entropy of this transition were determined to be $33.26 \pm 0.17\ \mathrm{kJ\,mol^{-1}}$ and $90.12 \pm 0.45\ \mathrm{J\,K^{-1}\,mol^{-1}}$, respectively. The standard thermodynamic functions $(H^0_T - H^0_{298.15})$ and $(S^0_T - S^0_{298.15})$, were derived from the heat capacity data in the temperature range of 80 to 390 K with an interval of 5 K. The standard molar enthalpy of combustion and the standard molar enthalpy of formation of the compound have been determined, $\Delta_c H^0_m$ ($C_5H_{12}O_5$, cr) = $(-2463.2 \pm 1.2)\ \mathrm{kJ\,mol^{-1}}$ and $\Delta_f H^0_m$ ($C_5H_{12}O_5$, cr) = $(-1219.3 \pm 0.3)\ \mathrm{kJ\,mol^{-1}}$, by means of a precision oxygen bomb combustion calorimeter at $T = 298.15$ K. DSC and TG measurements were performed to study the thermal stability of the compound. The results were in agreement with those obtained from heat capacity measurements.

Keywords: Xylitol; Heat capacity; Phase transition; Thermodynamic properties; Standard molar enthalpy of combustion; Standard molar enthalpy of formation; Adiabatic calorimetry; TG–DTG; DSC

1. Introduction

Xylitol [$(CH_2OH)(CHOH)_3(CH_2OH)$, CAS no. 87-99-0] is an important natural polyol in food and pharmaceutical applications, as it is increasingly used to provide sweetness to various products or replaces sugar in confectionery. Its molecular formula is $C_5H_{12}O_5$ with molar mass of 152.15 g mol^{-1} and structural formula as follows:

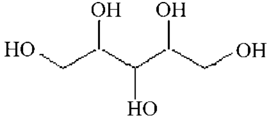

Compared with the sucrose, the xylitol has the characteristic sweet taste of sugars but the amount of energy (calories) in the products is reduced [1–3]. Another important advantage is that it does not contribute to the development of dental caries. Moreover, it is suitable for diabetics, because it does not require insulin of glucose in their metabolism [2,4]. In industrial applications, the state and phase transition of the xylitol affects its molecular mobility and physicochemical properties [5]. However, the thermodynamic properties of xylitol were scarcely reported. For the application and theoretical research concerned with the substance, the thermodynamic data of this compound are urgently needed.

Heat capacity is one of the most fundamental thermodynamic properties of substances and it closely related to other physical and chemical properties. Heat capacity determinations of various compounds have attracted many researchers. Adiabatic calorimetry is one of the most accurate method for obtaining the heat capacity, melting point and enthalpy of fusion of substances. In the present paper, low-temperature

---

[*] Corresponding author. Tel.: +86 411 84379199; fax: +86 411 84691570.
E-mail address: tzc@dicp.ac.cn (Z.-C. Tan).

doi:10.1016/j.tca.2007.02.022

heat capacity measurements were carried out with an adiabatic calorimeter over the temperature range from 80 to 390 K, and thermodynamic properties such as molar enthalpies and entropies of transition as well as chemical purity were determined based on the heat capacity measurements. The standard thermodynamic functions, $(H_T^0 - H_{298.15}^0)$ and $(S_T^0 - S_{298.15}^0)$, were calculated from heat capacity data in the temperature range of 80–390 K.

2. Experimental

2.1. Sample

The xylitol was purchased from ACROS ORGANICS company with labeled purity >99% mass fraction. The sample was recrystallized and then purified by sublimation. It was handled in a dry N_2 atmosphere to avoid possible contamination by moisture.

2.2. Adiabatic calorimetry

Heat capacity measurements were carried out in a high-precision automated adiabatic calorimeter described in detail in literature [6,7]. The calorimeter was established by Thermochemistry Laboratory of Dalian Institute of Chemical Physics, Chinese Academy of Sciences in PR China. It mainly consisted of a sample cell, a miniature platinum resistance thermometer, an electric heater, an inner and outer adiabatic shield, two sets of chromel–copel thermocouples and a high vacuum system. Its working temperature is from 80 to 400 K [8] with liquid nitrogen as cooling medium.

The measurements were conducted by means of the standard method of intermittently heating the sample and alternately measuring the temperature. The temperature difference between the sample and adiabatic shield was automatically kept to be about 10^{-3} K during the whole experiment. The temperature increment for a heating period was 2–4 K, and temperature drift was maintained about 10^{-4} K min^{-1} during each equilibrium period. The data were automatically collected through a Data Acquisition/Switch Unit (Model: 34420, Agilent, USA) and processed on line by a personal computer according to the program developed in our thermochemistry laboratory [9].

The sample amount used for the heat capacity measurement is 4.87213 g, which is equivalent to 32.022 m mol based on its molar mass of 152.15 g mol^{-1}.

2.3. DSC and TG analysis

A differential scanning calorimeter (Model: DSC141, SETARAM, France) was used to perform the thermal analysis of xylitol under high purity nitrogen (99.999%) with a flow rate of 40 ml min^{-1} and heating rate of 10 K min^{-1}. The mass of the sample used in the experiment was 3.48 mg.

The TG measurements of the sample were carried out by a thermogravimetric analyzer (Model: Setaram setsys 16/18, SETARAM, France) under N_2 with a flow rate of 40 ml min^{-1} and heating rate of 10 K min^{-1}. The mass of the sample used in the experiment was 8.35 mg.

2.4. Oxygen bomb combustion calorimetry

The constant-volume enthalpy of combustion of the sample was measured by means of a precision oxygen bomb combustion calorimeter, which was an isoperibolic calorimeter with a static oxygen bomb. The calorimeter was set up in our thermochemistry laboratory and the structure and principle of the calorimeter have been described previously in detail [10–12].

The sample of 0.6–0.9 g was pressed into pellets and put in a small sample crucible of about 0.004 dm^3, which was suspended in the bomb of about 0.3 dm^3, and burned under an oxygen pressure of 3.00 MPa ignited by a nickel fuse of about 16 cm. The purity of the oxygen used in the combustion was of research grade, mole fraction 0.99998. The real energy of combustion of the nickel fuse (Q_{Ni}) was calculated from the formula, Q_{Ni} $(J) = 2.929\Delta L$, in which ΔL (cm) was the length of the combusted nickel wire. The energy of formation of the aqueous nitric acid produced by oxidation of a trace of nitrogen, which contained in the oxygen bomb and produced from the combustion reaction, was determined by the neutral titration with a 0.08684 mol dm^{-3} of sodium hydroxide solution by using the phenolphthalein as the indicator. The enthalpy of formation of the aqueous nitric acid in the oxygen bomb can be derived from the equation, $Q_{\mathrm{HNO_3}}$ $(J) = 59.8NV$, in which N (mol dm^{-3}) is the concentration of the sodium hydroxide solution and V (dm^3) is the volume of the consumed sodium hydroxide solution; based on the molar enthalpy of formation of HNO_3(aq) from N_2(g), O_2(g) and H_2O(l), $\Delta_f H_m^0 = 59.8$ kJ mol^{-1} for 0.1 mol dm^{-3} of HNO_3(aq) [13,14].

3. Results and discussion

3.1. Heat capacity

Experimental molar heat capacities of xylitol measured by the adiabatic calorimeter over the temperature range from 80 to 390 K are listed in Table 1 and plotted in Fig. 1. From Fig. 1, a phase transition was observed in the range of 360–375 K with the peak heat capacity at 369.04 K. According to its melting point 365.7 K [15], this transition corresponds to a solid–liquid phase change.

The values of experimental heat capacities can be fitted to the following polynomial equations with least square method:

For the solid phase over the temperature range 80–360 K:

$$C_{p,\mathrm{m}}^0(\mathrm{J\,K^{-1}\,mol^{-1}}) = 165.87 + 105.19x + 1.8011x^2 - 41.445x^3 - 41.851x^4 + 65.152x^5 + 66.744x^6 \quad (1)$$

where x is the reduced temperature $x = [T - (T_{\max} + T_{\min})/2]/[(T_{\max} - T_{\min})/2]$, T the experimental tempera-

Table 1
Experimental molar heat capacity of xylitol ($M = 152.15\ \mathrm{g\,mol^{-1}}$)

T (K)	$C_{p,\mathrm{m}}^0$(J K^{-1} mol^{-1})	T (K)	$C_{p,\mathrm{m}}^0$(J K^{-1} mol^{-1})	T (K)	$C_{p,\mathrm{m}}^0$(J K^{-1} mol^{-1})
80.07	62.71	192.50	144.2	310.42	229.1
83.61	65.01	195.64	146.3	314.19	232.7
86.53	67.25	198.85	148.5	318.33	237.1
89.49	69.29	202.03	150.3	322.65	240.3
92.49	71.54	205.18	152.4	326.89	244.7
95.54	73.71	208.33	155.1	331.21	251.3
98.51	75.94	211.45	157.1	335.57	258.1
101.40	78.20	214.63	159.5	339.95	261.8
104.34	80.53	217.88	161.4	344.29	261.9
107.35	82.78	221.10	163.8	348.52	262.4
110.28	84.97	224.30	165.8	352.73	271.3
113.27	87.33	227.46	168.2	356.88	286.2
116.32	89.39	230.62	170.6	360.92	323.9
119.31	91.73	233.78	172.5	364.57	476.1
122.25	93.79	236.94	174.0	366.99	1196
125.24	96.15	240.13	176.1	368.02	3146
128.30	98.38	243.21	178.2	368.43	5878
131.31	100.5	246.34	180.8	368.64	8557
134.27	102.7	249.48	182.2	368.77	9597
137.29	104.8	252.61	184.3	368.82	10653
140.38	106.6	255.78	186.3	368.89	14023
143.41	109.0	258.93	188.6	368.91	18534
146.39	111.2	262.07	191.0	368.95	23261
149.42	113.3	265.19	193.2	368.98	24742
152.51	115.5	268.29	195.2	369.00	24741
155.56	117.7	271.44	197.5	369.02	25561
158.57	119.8	274.65	199.6	369.04	26128
161.56	121.9	277.84	201.9	369.06	24944
164.60	123.9	281.02	204.7	369.08	23799
167.69	126.0	284.19	207.3	369.10	22947
170.76	129.7	287.39	210.2	369.12	22657
173.84	132.3	290.63	212.7	370.05	837.0
176.88	134.0	293.83	215.1	372.89	422.0
179.99	136.0	297.06	217.8	376.72	424.4
183.16	138.0	300.40	220.6	380.91	427.0
186.30	140.4	303.70	223.9	385.11	428.8
189.41	142.5	307.01	226.5		

ture, thus, in the solid state (80–360 K), $x = [T\ (\mathrm{K}) - 220]/140$, $T_{\max}$ the upper limit (360 K) and $T_{\min}$ is the lower limit (80 K) of the above temperature region. The correlation coefficient of the fitting $R^2 = 0.9947$.

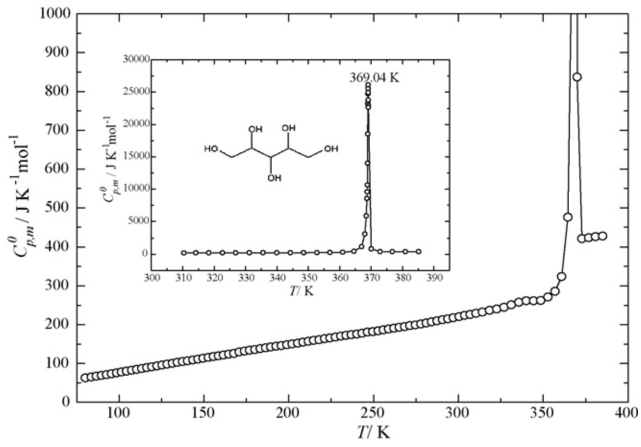

Fig. 1. Experimental molar heat capacity of xylitol as a function of temperature.

For the liquid phase over the temperature range 370–390 K:

$$C_{p,\mathrm{m}}^0(\mathrm{J\,K^{-1}\,mol^{-1}}) = 426.19 + 5.6366x \tag{2}$$

where x is the reduced temperature, $x = [T\ (\mathrm{K}) - 380]/10$, T is the experimental temperature, 380 obtained from polynomial $(T_{\max} + T_{\min})/2$, 10 obtained from polynomial $(T_{\max} - T_{\min})/2$. $T_{\max}$ and $T_{\min}$ are the upper (390 K) and lower (370 K) limit temperature, respectively. The correlation coefficient of the fitting $R^2 = 0.993$.

3.2. The temperature, enthalpy and entropy of solid–liquid phase transition

The standard molar enthalpy and entropy of the solid–liquid transition $\Delta_{\mathrm{fus}}H_{\mathrm{m}}^0$ and $\Delta_{\mathrm{fus}}S_{\mathrm{m}}^0$ of the compound were derived according to the following Eqs. (3) and (4):

$$\Delta_{\mathrm{fus}}H_{\mathrm{m}}^0 = \frac{Q - n\int_{T_i}^{T_\mathrm{m}} C_{p,\mathrm{m}}^0(\mathrm{s})\mathrm{d}T - n\int_{T_\mathrm{m}}^{T_\mathrm{f}} C_{p,\mathrm{m}}^0(\mathrm{l})\mathrm{d}T - \int_{T_\mathrm{i}}^{T_\mathrm{f}} H^0\,\mathrm{d}T}{n} \tag{3}$$

Table 2
Thermodynamic parameters of xylitol

Thermodynamic properties		Melting point T_m (K)	$\Delta_{\mathrm{fus}}H_{\mathrm{m}}^0$ (kJ mol^{-1})	$\Delta_{\mathrm{fus}}S_{\mathrm{m}}^0$ (J K^{-1} mol^{-1})
Present work	Adiabatic calorimetry	369.04	33.26 ± 0.17	90.12 ± 0.45
	DSC	367.52	33.68 ± 0.34	91.64 ± 0.90
Barone and Della Gatta [15]		365.7	37.40	102.3

$$\Delta_{\mathrm{fus}}S_{\mathrm{m}}^0 = \frac{\Delta_{\mathrm{fus}}H_{\mathrm{m}}^0}{T_{\mathrm{m}}} \qquad (4)$$

where T_{i} is the temperature that is somewhat lower than the temperature of the onset of a solid–liquid transition and T_{f} is the temperature slightly higher than that of the transition completion. Q the total energy introduced into the sample cell from T_{i} to T_{f}, H^0 the standard heat capacity of the sample cell from T_{i} to T_{f}, $C_{p,\mathrm{m}}^0(\mathrm{s})$ the standard heat capacity of the sample in solid phase from T_{i} to T_{m}, $C_{p,\mathrm{m}}^0(\mathrm{l})$ the standard heat capacity of the sample in liquid phase from T_{m} to T_{f} and n is molar amount of the sample. The heat capacity polynomials mentioned above were used to calculate the smoothed heat capacities, and were numerically integrated to obtain the values of the standard thermodynamic functions above $T = 298.15$ K. The calculated results are listed in Table 2.

3.3. Thermodynamic functions of the compound

The thermodynamic functions of the xylitol relative to the reference temperature 298.15 K were calculated in the temperature range 80–390 K with an interval of 5 K, using the polynomial equation of heat capacity and thermodynamic relationships as follows:

Before melting:

$$H_T^0 - H_{298.15}^0 = \int_{298.15}^{T} C_{p,\mathrm{m}}^0(\mathrm{s})\mathrm{d}T \qquad (5)$$

$$S_T^0 - S_{298.15}^0 = \int_{298.15}^{T} \frac{C_{p,\mathrm{m}}^0(\mathrm{s})}{T}\mathrm{d}T \qquad (6)$$

After melting:

$$H_T^0 - H_{298.15}^0 = \int_{298.15}^{T_{\mathrm{i}}} C_{p,\mathrm{m}}^0(\mathrm{s})\mathrm{d}T + \Delta_{\mathrm{fus}}H_{\mathrm{m}}^0 + \int_{T_{\mathrm{f}}}^{T} C_{p,\mathrm{m}}^0(\mathrm{l})\mathrm{d}T \qquad (7)$$

$$S_T^0 - S_{298.15}^0 = \int_{298.15}^{T} \left[\frac{C_{p,\mathrm{m}}^0(\mathrm{s})}{T}\right]\mathrm{d}T + \frac{\Delta_{\mathrm{fus}}H_{\mathrm{m}}^0}{T_{\mathrm{m}}} + \int_{T_{\mathrm{f}}}^{T} \left[\frac{C_{p,\mathrm{m}}^0(\mathrm{l})}{T}\right]\mathrm{d}T \qquad (8)$$

where T_{i} is the temperature at which the solid–liquid phase transition started; T_{f} the temperature at which the solid–liquid phase transition ended; $\Delta_{\mathrm{fus}}H_{\mathrm{m}}^0$ the standard molar enthalpy of fusion; T_{m} is the temperature of solid–liquid phase transition.

The standard thermodynamic functions, $H_T^0 - H_{298.15}^0$, $S_T^0 - S_{298.15}^0$, are listed in Table 3.

3.4. Constant-volume combustion energy, standard molar enthalpy of combustion, and standard enthalpy of formation

The constant-volume combustion energy of the organic compound can be calculated from the equation:

$$\Delta_{\mathrm{c}}U(\mathrm{J\,mol^{-1}}) = (\varepsilon_{\mathrm{calor}}\Delta T - Q_{\mathrm{Ni}} - Q_{\mathrm{HNO_3}})\frac{M}{W}$$

in which $\varepsilon_{\mathrm{calor}}$ (J K^{-1}) was the energy equivalent of the oxygen bomb calorimeter; ΔT (K) the corrected temperature rise; M (g mol^{-1}) the molar mass of the sample; W (g) is the mass of the sample. The results calculated by the equation were listed in Table 4.

The standard molar enthalpy of combustion of the organic compound, $\Delta_{\mathrm{c}}H_{\mathrm{m}}^0$, referred to the combustion enthalpy change of the following reaction at $T = 298.15$ K and $P^0 = 100.325$ kPa based on the definition of the combustion enthalpy of the organic compound:

$$\mathrm{C_5H_{12}O_5(cr)} + 11/2\mathrm{O_2(g)} = 5\mathrm{CO_2(g)} + 6\mathrm{H_2O(l)} \qquad (9)$$

The standard molar enthalpies of combustion can be derived from the constant-volume combustion energy by means of the following formula:

$$\Delta_{\mathrm{c}}H_{\mathrm{m}}^0 = \Delta_{\mathrm{c}}U_{\mathrm{m}} + \Delta nRT$$

$$\Delta n = \sum n_i(\text{products, g}) - \sum n_i(\text{reactants, g})$$

where $\sum n_i$ was the total molar amount of the gases in products or reactants. The calculated standard molar enthalpy of combustion of the organic compound was

$$\Delta_{\mathrm{c}}H_{\mathrm{m}}^0(\mathrm{C_5H_{12}O_5, cr}) = -2463.2 \pm 1.2\,\mathrm{kJ\,mol^{-1}}$$

The standard molar enthalpy of formation of the organic compound, $\Delta_{\mathrm{f}}H_{\mathrm{m}}^0$, was calculated by a designed Hess thermochemical cycle according to the reaction (9) as follows:

$$\Delta_{\mathrm{f}}H_{\mathrm{m}}^0(\mathrm{C_5H_{12}O_5, cr}) = [5\Delta_{\mathrm{f}}H_{\mathrm{m}}^0(\mathrm{CO_2, g}) + 6\Delta_{\mathrm{f}}H_{\mathrm{m}}^0(\mathrm{H_2O, l})] - \Delta_{\mathrm{c}}H_{\mathrm{m}}^0(\mathrm{C_5H_{12}O_5, cr})$$

In the above formula, the standard molar enthalpies of formation of $\mathrm{CO_2(g)}$ and $\mathrm{H_2O(l)}$, recommended by CODATA [12,13], $\Delta_{\mathrm{f}}H_{\mathrm{m}}^0(\mathrm{CO_2, g}) = -393.51 \pm 0.13\,\mathrm{kJ\,mol^{-1}}$, $\Delta_{\mathrm{f}}H_{\mathrm{m}}^0(\mathrm{H_2O, l}) = -285.83 \pm 0.04\,\mathrm{kJ\,mol^{-1}}$, were employed in the calculation of $\Delta_{\mathrm{f}}H_{\mathrm{m}}^0(\mathrm{C_5H_{12}O_5, cr})$ values. Based on these values and the standard molar enthalpy of combustion, the standard molar

Table 3
Calculated thermodynamic functions of xylitol

T (K)	$C^0_{p,m}$ ($\mathrm{J\,K^{-1}\,mol^{-1}}$)	$H^0_T - H^0_{298.15}$ ($\mathrm{kJ\,mol^{-1}}$)	$S^0_T - S^0_{298.15}$ ($\mathrm{J\,K^{-1}\,mol^{-1}}$)
80	63.67	−31.17	−164.2
85	66.43	−30.85	−160.3
90	69.62	−30.51	−156.4
95	73.13	−30.15	−152.5
100	76.86	−29.78	−148.6
105	80.73	−29.38	−144.8
110	84.68	−28.97	−140.9
115	88.65	−28.53	−137.1
120	92.61	−28.08	−133.3
125	96.54	−27.61	−129.4
130	100.4	−27.12	−125.6
135	104.2	−26.60	−121.8
140	108.0	−26.07	−118.0
145	111.7	−25.52	−114.2
150	115.3	−24.96	−110.4
155	118.9	−24.37	−106.6
160	122.4	−23.77	−102.8
165	126.0	−23.15	−98.98
170	129.5	−22.51	−95.20
175	133.0	−21.85	−91.43
180	136.6	−21.18	−87.67
185	140.1	−20.49	−83.91
190	143.7	−19.78	−80.16
195	147.3	−19.05	−76.41
200	151.0	−18.30	−72.67
205	154.7	−17.54	−68.93
210	158.4	−16.76	−65.19
215	162.1	−15.96	−61.45
220	165.9	−15.14	−57.72
225	169.6	−14.30	−54.00
230	173.4	−13.44	−50.27
235	177.1	−12.56	−46.54
240	180.8	−11.67	−42.82
245	184.4	−10.76	−39.10
250	188.0	−9.824	−35.39
255	191.5	−8.875	−31.68
260	195.0	−7.909	−27.98
265	198.3	−6.926	−24.28
270	201.6	−5.926	−20.60
275	204.8	−4.910	−16.92
280	208.0	−3.878	−13.25
285	211.1	−2.830	−9.586
290	214.2	−1.767	−5.934
295	217.4	−0.6879	−2.291
298.15	219.4	0	0
300	220.7	0.4071	1.345
305	224.2	1.519	4.976
310	227.9	2.649	8.607
315	232.1	3.799	12.24
320	236.9	4.972	15.89
325	242.4	6.169	19.56
330	248.8	7.397	23.26
335	256.3	8.659	27.00
340	265.3	9.963	30.81
345	275.9	11.31	34.70
350	288.6	12.73	38.70
355	303.6	14.20	42.84
360	321.5	15.77	47.15
365	Phase change	–	–
370	420.6	50.30	140.8
375	423.4	52.41	146.4
380	426.2	54.53	152.1
385	429.0	56.67	157.6
390	431.8	58.82	163.2

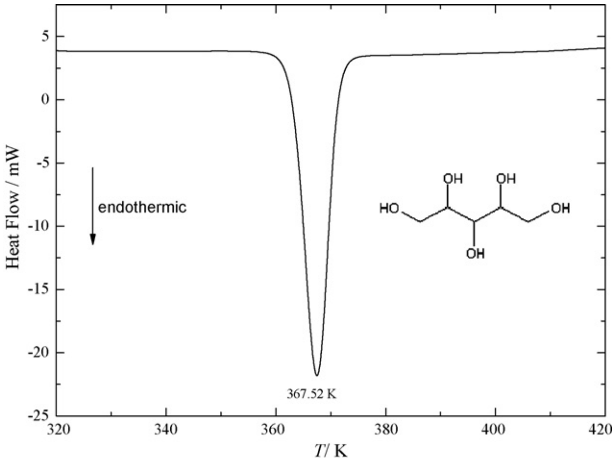

Fig. 2. DSC curve of xylitol under high purity nitrogen.

enthalpy of formation of xylitol can be calculated to be: $\Delta_f H^0_m(C_5H_{12}O_5, \mathrm{cr}) = -1219.3 \pm 0.31\,\mathrm{kJ\,mol^{-1}}$.

3.5. The result of TG and DSC analysis

From the DSC curve in Fig. 2, a sharply endothermic peak corresponding to melting process was observed, with the peak temperature of 367.52 K and the enthalpy of $33.68 \pm 0.34\,\mathrm{kJ\,mol^{-1}}$, which are consistent with the values (369.04 K, $33.26 \pm 0.17\,\mathrm{kJ\,mol^{-1}}$) observed from the adiabatic calorimetric measurements. The results were listed in Table 2, from which, it can be seen that the standard thermodynamic parameters obtained from adiabatic calorimetry and DSC in the present research are in accordance with each other and slightly lower than those reported in literature [15].

From the TG curve in Fig. 3, it can be seen that the mass loss of the sample was completed in a single step. The sample keeps thermostable below 400 K. It begins to lose weight at 451.20 K, reaches the maximum rate of weight loss at 617.13 K and completely loses its weight when the temperature reaches 675.30 K.

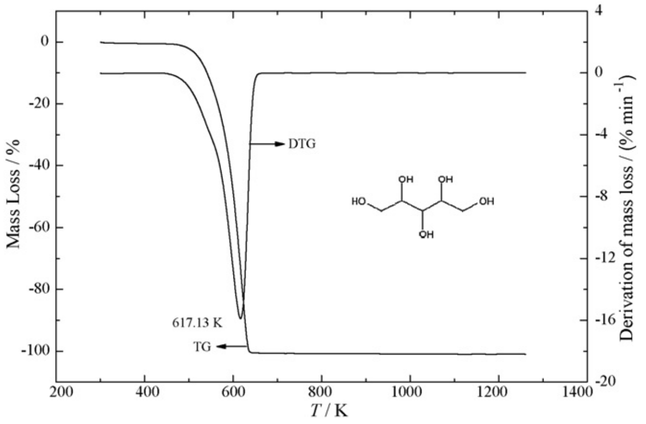

Fig. 3. TG–DTG curve of xylitol under high purity nitrogen.

Table 4
Experimental results of constant-volume combustion energy for xylitol

No.	Sample mass (mg)	Heat value of nickel wire Q_{Ni} (J)	Heat value of nitric acid $Q_{\mathrm{HNO_3}}$ (J)	Corrected temperature rise ΔT (K)	Combustion energies, ΔU_c (kJ mol^{-1})
1	0.87110	27.8236	30.0313	1.3357	2468.6
2	0.59009	30.7524	18.7046	1.0472	2461.7
3	0.61246	36.6100	21.5623	1.0979	2464.0
4	0.62906	22.6014	38.9530	1.0831	2462.7
5	0.62042	23.7233	20.2633	0.9644	2459.9
6	0.63957	41.8818	23.6405	1.1741	2462.1
Avg. $\Delta U_c = (\overline{\Delta U_c} \pm \sigma *) = -2463.2 \pm 1.2$					

* $\sigma = \sqrt{\Sigma_{i=1}^{n}(x_i - \bar{x})^2/n(n-1)}$, in which n is the experimental number ($n = 6$); x_i a single value of combustion energies; $\bar{x}$ is the mean value of combustion energies.

3.6. Purity determination of the sample

Adiabatic calorimetry provides an accurate way for determining the purity of a substance. Here, we suppose that the impurity resolves ideally in the liquid phase of the sample and does not resolve at all in the solid phase. The total amount of impurities does not exceed a couple of mole%. According to the ideal solution law, the relation between the mole fraction N ($N \ll 1$) of a small amount of impurities in the sample and its melting point depression is as follows:

$$N = \frac{\Delta H_{\mathrm{m}}(T_0 - T_1)}{RT_0^2} \tag{10}$$

where T_0 is the melting point of an absolutely pure substance; T_1 the melting point of the given sample, ΔH_{m} the heat of fusion of the sample and R is molar gas constant. As for the liquid solution formed by a part of the sample melted, given that $N'$is the mole fraction of the impurities and T is the melting point of the solution, then

$$N' = \frac{\Delta H_{\mathrm{m}}(T_0 - T)}{RT_0{}^2} \tag{11}$$

If it is assumed that the impurities are solid-insoluble and all of the impurities are transferred completely into the liquid phase when the melting started, the relative amount of the sample in the liquid phase will be increasingly more in the process of the melting; on the other hand, since the total amount of the impurities remains constant, the mole fraction of the impurities in the liquid phase will gradually decrease. Given: F is the ratio of the amount of the sample in the liquid phase to the total amount of the sample, then

$$F = q/Q \tag{12}$$

where F is also designated as the fraction melted, its value being the ratio of the heat required to melt a part of the sample (q) to the total heat required to melt the whole sample (Q). Obviously, F is inversely proportional to the mole fraction of the impurities in the liquid phase, that is

$$N' = \frac{1}{F}N \tag{13}$$

Table 5
Experimental values of melted fraction (F) and equilibrium temperature (T) of xylitol

$F = q/Q$	$1/F$	T (K)
0.128	7.78	368.77
0.224	4.46	368.89
0.321	3.12	368.95
0.428	2.33	369.00
0.537	1.86	369.04

Substituting Eqs. (10) and (11) into (13), we have

$$T_0 - T = \frac{1}{F}(T_0 - T_1) \tag{14}$$

From (14) it may be observed that the relation between the melting point, or the equilibrium melting temperature T and $1/F$ is linear. The purity of the sample was determined by a set of equilibrium melting temperatures (T) and melting fractions (F) corresponding to these temperatures [16–18]. The calculated results are shown in Table 5. A plot of the equilibrium melting temperature (T) versus the reciprocal of the melting fractions ($1/F$) is a straight line, as shown in Fig. 4. The T_0 is the temperature when $1/F$ is 0 and T_1 is the temperature when $1/F$ equals to 1. From Fig. 4, the T_0 = 369.10 K and T_1 = 369.06 K were obtained, respectively. Thus, we calculated the mol percentage of impuri-

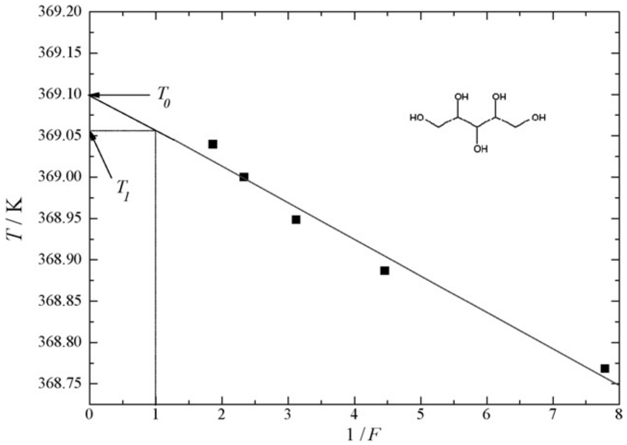

Fig. 4. Melting curve of xylitol with temperature plotted against reciprocal of the melting fraction (T_0 = 369.10 K, T_1 = 369.06 K).

ties, $N = 1.298 \times 10^{-3}$ mol fraction from Eq. (10), and the purity of the sample amounted to $1 - N = 0.9987$ mol fraction.

4. Conclusions

The heat capacities of xylitol were measured in the temperature range from 80 to 390 K by a high-precision automated adiabatic calorimeter. From the results of heat capacity experiment, the thermodynamic properties of fusion were completely studied, and the thermodynamic functions $(H_T^0 - H_{298.15}^0)$ and $(S_T^0 - S_{298.15}^0)$ were derived in the range from 80 to 390 K with temperature interval of 5 K. The melting temperature, standard molar enthalpy and entropy of this transition were determined to be 369.04 K, 33.26 ± 0.17 kJ mol^{-1} and 90.12 ± 0.45 J K^{-1} mol^{-1}, respectively. The chemical purity was calculated to be 0.9987 mol fraction according to the Van't Hoff equation. The standard molar enthalpy of formation of xylitol was derived to be -1219.3 ± 0.3 kJ mol^{-1} with a precision oxygen bomb combustion calorimeter.

Acknowledgements

This work was financially supported by the National Nature Science Foundation of China under the grant NSFC no. 20373072.

References

[1] N.C.L.A.V. Gonçalves, A.A. Del Bel Cury, G.S. Simo es, A.T. Hara, P.L. Rosalen, J.A. Cury, J. Dent. 34 (2006) 662–667.
[2] J. Goossens, M. Gonze, Manuf. Confect. 80 (2000) 71.
[3] J.M. deMan, Principles of Food chemistry, Aspen Publication, Gaithersurg, MD, 1999, p. 181.
[4] R.L. Whistler, J.N. BeMiller, Carbohydrate Chemistry for Food Scientists, Eagan Press, St. Paul, MN, 1997, p. 23.
[5] R.A. Talja, Y.H. Roos, Thermochim. Acta 380 (2001) 109–121.
[6] Z.C. Tan, G.Y. Sun, Y. Sun, J. Therm. Anal. 45 (1995) 59–67.
[7] Z.C. Tan, G.Y. Sun, Y.J. Song, Thermochim. Acta 252–253 (2000) 247–253.
[8] Z.C. Tan, L.X. Sun, S.H. Meng, J. Chem. Thermodyn. 34 (2002) 1417–1429.
[9] Z.C. Tan, B.P. Liu, J.B. Yan, L.X. Sun, Comput. Appl. Chem. 20 (2003) 264.
[10] Y.Y. Di, Z.C. Tan, X.H. Sun, M.H. Wang, F. Xu, Y.F. Liu, L.X. Sun, H.T. Zhang, J. Chem. Thermodyn. 36 (2004) 79–86.
[11] L.M. Zhang, Z.C. Tan, S.D. Wang, D.Y. Wu, Thermochim. Acta 299 (1997) 13–17.
[12] X.M. Wu, Z.C. Tan, S.H. Meng, C.X. Sun, F.D. Wang, S.S. Qu, Thermochim. Acta 359 (2000) 103–107.
[13] A.R. Aguilar, E.O. Guareno, J. Chem. Thermodyn. 32 (2000) 767–775.
[14] S.V. Melkhanova, S.M. Pimenova, V.P. Kolesov, A.A. Pimerzin, V.S. Sarkisova, J. Chem. Thermodyn. 32 (2000) 1311–1317.
[15] G. Barone, G. Della Gatta, J. Chem. Soc. Faraday Trans. 86 (1) (1990) 75–79.
[16] B.P. Liu, Z.C. Tan, J.L. Lu, X.Z. Lan, L.X. Sun, F. Xu, P. Yu, J. Xing, Thermochim. Acta 397 (2003) 67.
[17] Y.Y. Di, Z.C. Tan, X.M. Wu, S.H. Meng, S.S. Qu, Thermochim. Acta 356 (2000) 143.
[18] Z.C. Tan, J.C. Yie, X.A. Yin, S.X. Chen, W.B. Wang, Chin. Sci. Bull. 32 (1987) 240.